A Comparative Study of the Boundary Control of Buck Converters Using First- and Second-Order Switching Surfaces -Part II: Discontinuous Conduction Mode

Kelvin K. S. Leung and Henry S. H. Chung†

Department of Electronic Engineering
City University of Hong Kong
Tat Chee Avnue, Kowloon Tong, Kowloon, Hong Kong SAR, China
†Email: eeshc@cityu.edu.hk

Abstract—This paper extends the scope of the Part-I companion paper on comparing the performance characteristics of buck converters with the first- (σ^1) and second-order (σ^2) switching surfaces. Major emphasis is given to converters operating in discontinuous conduction mode (DCM). Similar to the companion paper, performance attributes under investigation in this paper includes the average output voltage, output ripple voltage, switching frequency, parametric sensitivities to the component values, and large-signal characteristics. Due to the presence of the output hysteresis band, an additional switching boundary formed by the zero-inductor-current trajectory is created. This phenomenon causes a shift of the operating point in converters with σ^1. Conversely, the operating point remains unchanged in converters with σ^2. As well as in continuous conduction mode (CCM), σ^2 can make the converter revert to the steady state in two switching cycles in DCM and gives better static and dynamic responses than σ^1 in both CCM and DCM. Most importantly, its control law and settings are the same in both modes. Experimental results of a prototype are found to be in good agreement with theoretical predictions.

I. INTRODUCTION

Most research articles on discussing the boundary control of switching dc/dc converters focus on the static and dynamic behaviors of converters operating in continuous conduction mode [1]-[2]. The hysteresis band is usually assumed to be zero in those analyses. There is limited information on the characteristics of converters operating in discontinuous conduction mode (DCM). As expressed in eqs. (31) and (46) in [3], the critical resistances of the buck converters with σ^1 and σ^2 theoretically tend to infinity with zero hysteresis band and thus DCM does not occur for a large-signal stable switching surface. However, as shown in eqs. (51) and (53) in [3], the switching frequency will also tend to infinitive. Thus, a hysteresis band will usually be introduced to limit the switching frequency. With nonzero hysteresis band, an additional switching boundary formed by zero-inductor-current trajectory is created and possibly makes the converter enter into DCM. Fig. 1(a) depicts the state trajectories and Fig. 1(b) shows the time-domain output voltage and inductor current waveforms of converters in DCM with σ^1. The output capacitor discharges to the load and the trajectory will move along the x-axis, when the main switch and the diode are off. This results in a shift of the average output voltage. Fig. 2(a) illustrates the output voltage shift when the output load is changed from R_1 to R_2, where $R_2 > R_{crit}^{<1>} > R_1$ and $R_{crit}^{<1>}$ is the critical resistance. The operating point is shifted from 'O_1' (when the load is R_1) to a new operating point 'O_2' (when the load is R_2). When the load is R_1,

The work described in this paper was fully supported by a Strategic Research Grant from the City University of Hong Kong (Project No.: 7001595).

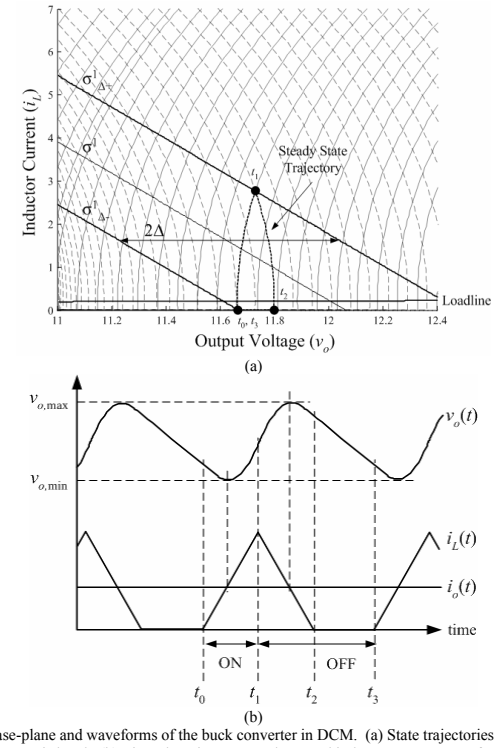

Fig. 1 Phase-plane and waveforms of the buck converter in DCM. (a) State trajectories with nonzero hysteresis band. (b) Time-domain output voltage and inductor current waveforms.

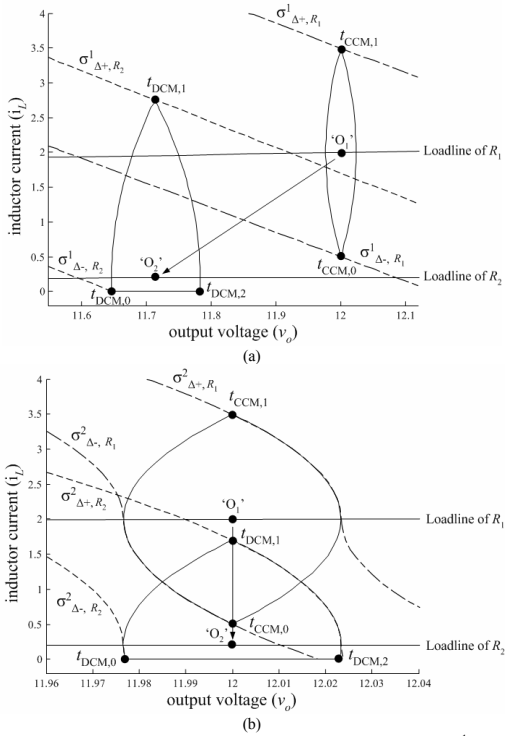

Fig. 2 Shift of operating point of the converter in DCM with different loads. (a) σ^1. (b) σ^2.

the converter operates in CCM. The average output voltage is close to the reference voltage v_{ref}, as expressed in eq. (29) in [3]. However, when the load is R_2, the average output will move away from v_{ref}.

For converters with σ^2, the operating point remains unchanged. Fig. 2(b) shows the state trajectories when the load is changed from R_1 to R_2. In this respect, σ^2 exhibits a better static behavior than σ^1. This paper extends the scope of the Part-I companion paper on comparing the performance characteristics of buck converters with the first- (σ^1) and second-order (σ^2) switching surfaces. Similar to the companion paper, performance attributes under investigation includes the average output voltage, output ripple voltage, switching frequency, parametric sensitivities to the component values, and large-signal characteristics. The effect of the equivalent series resistance of the output capacitor on the operating mode will be discussed. As well as in CCM, σ^2 also provides better dynamic responses than σ^1 for converters operating in DCM. Ideally, it can make the converter revert to the steady state in two switching actions under large-signal disturbances. Most importantly, the control law and setting of σ^2 are the same in both CCM and DCM. Experimental results of a prototype are found to be in good agreement with theoretical predictions.

II. Definitions and Formulas

The basic definitions and formulas in [3] are used in the following analysis. The converter can be described by the state-space equation of

$$\begin{aligned} \dot{x} &= A_0\, x + B_0\, u + (A_1\, x + B_1\, u)\, q_1 + (A_2\, x + B_2\, u)\, q_2 \\ y &= C\, x \end{aligned} \tag{1}$$

where $x = [i_L\ v_C]$, $y = v_o$, A_i, B_i, and C are constant matrices, and q_i represents the state of the switch S_i. If S_i is on, $q_i = 1$, and vice versa. S_1 represents the main switch and S_2 represents the diode. Matrices A_0, B_0, A_1, B_1, A_2, and B_2 are defined as

$$A_0 = \begin{bmatrix} 0 & 0 \\ 0 & -\dfrac{1}{C(R+r_C)} \end{bmatrix},\quad B_0 = \begin{bmatrix} 0 \\ 0 \end{bmatrix},\quad A_1 = A_2 = \begin{bmatrix} -\dfrac{Rr_C}{L(R+r_C)} & -\dfrac{R}{L(R+r_C)} \\ \dfrac{R}{C(R+r_C)} & 0 \end{bmatrix},\quad B_1 = \begin{bmatrix} \dfrac{1}{L} \\ 0 \end{bmatrix},$$

$$B_2 = \begin{bmatrix} 0 \\ 0 \end{bmatrix} \text{ and } C = \begin{bmatrix} \dfrac{Rr_C}{R+r_C} & \dfrac{R}{R+r_C} \end{bmatrix}.$$

A. On- and Off-State Trajectories

When S_1 is on and S_2 is off, the on-state trajectory $\{v_{o,on}, i_{L,on}\}$ is

$$\begin{aligned} v_{o,on} = {} & \frac{L}{2C(v_i - v_{ref})}\left(\left(i_{L,on} - \frac{v_{o,on}}{R}\right)^2 - \left(i_{L,0} - \frac{v_{o,0}}{R}\right)^2\right) + v_{o,0} \\ & + r_C\left(\left(i_{L,on} - \frac{v_{o,on}}{R}\right) - \left(i_{L,0} - \frac{v_{o,0}}{R}\right)\right) \end{aligned} \tag{2}$$

where $i_{L,0}$ and $v_{o,0}$ are the initial values of i_L and v_o, respectively, in this stage.

When S_1 is off and S_2 is on, the off-state trajectory $\{v_{o,off}, i_{L,off}\}$ is

$$\begin{aligned} v_{o,off} = {} & -\frac{L}{2Cv_{ref}}\left(\left(i_{L,off} - \frac{v_{o,off}}{R}\right)^2 - \left(i_{L,1} - \frac{v_{o,1}}{R}\right)^2\right) + v_{o,1} \\ & + r_C\left(\left(i_{L,off} - \frac{v_{o,off}}{R}\right) - \left(i_{L1} - \frac{v_{o,1}}{R}\right)\right) \end{aligned} \tag{3}$$

where $i_{L,1}$ and $v_{o,1}$ are the initial values of i_L and v_o, respectively, in this stage.

When both S_1 and S_2 are off, the trajectory moves along the x-axis and $i_L = 0$.

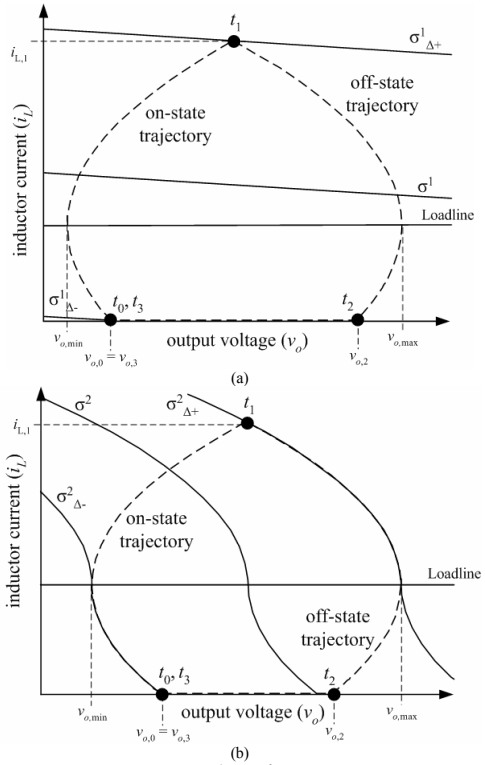

Fig. 3 Steady-state trajectories in DCM. (a) σ^1. (b) σ^2.

B. Modeling of σ^1 and σ^2

The general form of σ^1 can be written as

$$\sigma^1{}_{\Delta+} = c_1\left(i_L - \frac{v_o}{R}\right) + \left(v_o - \left(v_{ref} + \Delta_1\right)\right) = 0 \tag{4}$$

$$\sigma^1{}_{\Delta-} = c_1\left(i_L - \frac{v_o}{R}\right) + \left(v_o - \left(v_{ref} - \Delta_1\right)\right) = 0 \tag{5}$$

where c_1 is a constant and v_{ref} is the reference output. i_L and v_o are in a linear relationship.

The general form of σ^2 is defined as

$$\sigma^2{}_{\Delta+} = k_1\left(i_L - \frac{v_o}{R}\right)^2 + \left(v_o - \left(v_{ref} + \Delta_2\right)\right), \quad \left(i_L - \frac{v_o}{R}\right) > 0 \tag{6}$$

$$\sigma^2{}_{\Delta-} = -k_2\left(i_L - \frac{v_o}{R}\right)^2 + \left(v_o - \left(v_{ref} - \Delta_2\right)\right), \quad \left(i_L - \frac{v_o}{R}\right) < 0 \tag{7}$$

where k_1 and k_2 are constants.

If $r_C = 0$, the ideal values of k_1 and k_2 are

$$\{k_1, k_2\} = \left\{\frac{L}{2C\,v_{ref}}, \frac{L}{2C\,(v_i - v_{ref})}\right\} \tag{8}$$

C. Average Output Voltage and Output Ripple Voltage

The average output voltage v_{avg} is defined as the mean of the minimum output voltage $v_{o,\min}$ and the maximum output voltage $v_{o,\max}$. That is,

$$v_{avg} = \frac{v_{o,\min} + v_{o,\max}}{2} \tag{9}$$

The output ripple voltage v_{ripple} is defined as

$$v_{ripple} = v_{o,\max} - v_{o,\min} \tag{10}$$

III. Steady-State Characteristics

Fig. 3(a) and (b) show the trajectory with σ^1 and σ^2 in DCM, respectively, with $r_C = 0$,

$$v_{o,0} = v_{o,3} \tag{11}$$

and

$$i_{L,0} = i_{L,3} \tag{12}$$

where $v_o(t_0) = v_{o,0}$, $v_o(t_3) = v_{o,3}$, $i_L(t_0) = i_{L,0}$ and $i_L(t_3) = i_{L,3}$.

In DCM, both S_1 and S_2 are off from t_2 to t_3, therefore,

$$i_{L,0} = i_{L,2} = i_{L,3} = 0 \tag{13}$$

where $i_L(t_2) = i_{L,2}$.

By putting (11)-(13) into (2),

$$v_{o,1} = \frac{L}{2C(v_i - v_{ref})}\left(\left(i_{L,1} - \frac{v_{o,1}}{R}\right)^2 - \left(\frac{v_{o,0}}{R}\right)^2\right) + v_{o,0} \tag{14}$$

where $v_o(t_1) = v_{o,1}$, $i_L(t_1) = i_{L,1}$.

Similarly, by putting (11)-(13) into (3),

$$v_{o,2} = -\frac{L}{2C v_{ref}}\left(\left(\frac{v_{o,2}}{R}\right)^2 - \left(i_{L,1} - \frac{v_{o,1}}{R}\right)^2\right) + v_{o,1} \tag{15}$$

where $v_o(t_2) = v_{o,2}$.

A. Average Output Voltage and Output Ripple Voltage

1. σ^1

As derived in eq. (31) in [3], the converter is in critical mode, when

$$R = R_{crit}^{<1>} = \frac{v_{ref}\ c_1}{\Delta_1} \tag{16}$$

where $R_{crit}^{<1>}$ is the critical load resistance for $r_C = 0$.

By putting (13) into (4) and (5), they give

$$\sigma^1{}_{\Delta+} = c_1\left(i_{L,1} - \frac{v_{o,1}}{R}\right) + \left(v_{o,1} - \left(v_{ref} + \Delta_1\right)\right) = 0 \tag{17}$$

$$\sigma^1{}_{\Delta-} = c_1\left(-\frac{v_{o,0}}{R}\right) + \left(v_{o,0} - \left(v_{ref} - \Delta_1\right)\right) = 0 \tag{18}$$

By rearranging (18),

$$v_{o,0} = \frac{R}{R - c_1}\left(v_{ref} - \Delta_1\right) \tag{19}$$

By using (17) and (19) to solve (14),

$$v_{o,1} = v_{ref} + \Delta_1 - \Psi_1 \tag{20}$$

where $\Psi_1 = \frac{\sqrt{1 + 8\alpha\Delta_1 - 4\Phi_1\alpha} - 1}{2\alpha}$, $\alpha = \frac{L}{2C{c_1}^2\left(v_i - v_{ref}\right)}$,

$\Phi_1 = \frac{c_1}{R - c_1}\left(v_{ref} - \Delta_1\right)\left(1 - \frac{c_1\alpha\left(v_{ref} - \Delta_1\right)}{R - c_1}\right)$.

By substituting (20) into (17), it can be shown that

$$i_{L,1} = \frac{v_{ref} + \Delta_1 - \Psi_1}{R} + \frac{\Psi_1}{c_1} \tag{21}$$

By substituting (20) and (21) into (15), it can be shown that

$$v_{o,2} = \frac{C R^2 v_{ref}}{L}\left(-1 + \sqrt{1 + \frac{2L}{C R^2 v_{ref}}\left(v_{ref} + \Delta_1 - \Psi_1 + \frac{L}{2C{c_1}^2 v_{ref}}{\Psi_1}^2\right)}\right) \tag{22}$$

As shown in eqs. (25) and (27) in [3], $v_{o,\max}$ and $v_{o,\min}$ can be derived as

$$v_{o,\max} = v_{o,1} + \frac{L}{2\ C\ v_{ref}}\left(i_{L,1} - \frac{v_{o,1}}{R}\right)^2 \tag{23}$$

$$v_{o,\min} = v_{o,0} - \frac{L}{2C\left(v_i - v_{ref}\right)}\left(i_{L,0} - \frac{v_{o,0}}{R}\right)^2 \tag{24}$$

By using (20) and (21), equation (23) can be expressed as,

$$v_{o,\max} = v_{ref} - \Delta_1 + \Phi_1 + \frac{v_i\,\alpha}{v_{ref}}{\Psi_1}^2 \tag{25}$$

By using (13) and (19), equation (24) can be expressed as,

$$v_{o,\min} = v_{ref} - \Delta_1 + \Phi_1 \tag{26}$$

Thus, by putting (25) and (26) into (9),

$$v_{avg} = v_{ref} - \Delta_1 + \Phi_1 + \frac{v_i\,\alpha}{2v_{ref}}{\Psi_1}^2 \tag{27}$$

Thus, the value of v_{avg} with σ^1 is dependent on Δ_1.

By putting (25) and (26) into (10), it can be shown that

$$v_{ripple} = \frac{v_i\,\alpha}{v_{ref}}{\Psi_1}^2 \tag{28}$$

When $R \to \infty$ and $\Phi_1 \to 0$,

$$v_{avg} = v_{ref} - \Delta_1 + \frac{v_i}{8v_{ref}\,\alpha}\left(\sqrt{1 + 8\alpha\Delta_1} - 1\right)^2 \tag{29}$$

$$v_{ripple} = \frac{v_i}{4v_{ref}\,\alpha}\left(\sqrt{1 + 8\alpha\Delta_1} - 1\right)^2 \tag{30}$$

2. σ^2

As derived in eq. (46) in [3], the converter is in critical mode, when

$$R = R_{crit}^{<2>} = \frac{v_{ref} - \frac{k_1 - k_2}{k_1 + k_2}\Delta_2}{\sqrt{\frac{2\Delta_2}{k_1 + k_2}}} \tag{31}$$

where $R_{crit}^{<2>}$ is the critical load resistance for $r_C = 0$.

By putting (13) into (6) and (7),

$$\sigma^2{}_{\Delta+} = k_1\left(i_{L,1} - \frac{v_{o,1}}{R}\right)^2 + \left(v_{o,1} - \left(v_{ref} + \Delta_2\right)\right) = 0 \tag{32}$$

$$\sigma^2{}_{\Delta-} = -k_2\left(\frac{v_{o,0}}{R}\right)^2 + \left(v_{o,0} - \left(v_{ref} - \Delta_2\right)\right) = 0 \tag{33}$$

By solving (33) for $v_{o,0}$, it gives

$$v_{o,0} = \frac{R^2}{2k_2}\left(1 - \sqrt{1 - \frac{4k_2}{R^2}\left(v_{ref} - \Delta_2\right)}\right) \tag{34}$$

By solving (14) with (32) and (34), it gives

$$v_{o,1} = v_{ref} + \Delta_2 - \Psi_2 \tag{35}$$

where $\Psi_2 = \frac{2\Delta_2 - \Phi_2}{1 + \beta}$, $\beta = \frac{L}{2C k_1\left(v_i - v_{ref}\right)}$,

$\Phi_2 = \left(k_2 - \beta k_1\right)\left(\frac{R}{2k_2}\left(1 - \sqrt{1 - \frac{4k_2}{R^2}\left(v_{ref} - \Delta_2\right)}\right)\right)^2$.

By substituting (35) into (32), it can shown that

$$i_{L,1} = \frac{v_{ref} + \Delta_2 - \Psi_2}{R} + \sqrt{\frac{\Psi_2}{k_1}} \tag{36}$$

By substituting (35) and (36) into (15), it can shown that

$$v_{o,2} = \frac{C R^2 v_{ref}}{L}\left(-1 + \sqrt{1 + \frac{2L}{C R^2 v_{ref}}\left(v_{ref} + \Delta_2 - \Psi_2 + \frac{L}{2C v_{ref} k_1}\Psi_2\right)}\right) \tag{37}$$

By using (35) and (36), equation (23) can be expressed as,

$$v_{o,\max} = v_{ref} - \Delta_2 + \Phi_2 + \frac{v_i\,\beta}{v_{ref}}\Psi_2 \tag{38}$$

By using (13) and (34), equation (24) can be expressed as,

$$v_{o,\min} = v_{ref} - \Delta_2 + \Phi_2 \tag{39}$$

By substituting (38) and (39) into (9), it can shown that

$$v_{avg} = v_{ref} - \Delta_2 + \Phi_2 + \frac{v_i\,\beta}{2v_{ref}}\Psi_2 \tag{40}$$

By putting (38) and (39) into (10),

$$v_{ripple} = \frac{v_i\,\beta}{v_{ref}}\Psi_2 \tag{41}$$

When $R \to \infty$ and $\Phi_2 \to 0$,

$$v_{avg} = v_{ref} - \Delta_2 + \frac{\beta}{1 + \beta}\frac{v_{in}}{v_{ref}}\Delta_2 \tag{42}$$

$$v_{ripple} = \frac{2\beta}{1+\beta}\frac{v_i}{v_{ref}}\Delta_2 \tag{43}$$

With the ideal values of k_1 and k_2 in (8),

$$v_{avg} = v_{ref} \tag{44}$$

$$v_{ripple} = 2\Delta_2 \tag{45}$$

for $R > R_{crit}^{<2>}$. It can be noted that v_{avg} is independent on Δ_2.

C. Switching Frequency

In DCM, $i_{L,0} = i_{L,2} = i_{L,3} = 0$ and $v_{o,0} = v_{o,3}$. For $r_C = 0$, the average output current I_o can be expressed as,

$$I_o = \bar{i}_L = \frac{1}{T_S}\int_{t_0}^{t_3} i_L\,dt = \frac{1}{T_S}\left(\int_{t_0}^{t_1} i_L\,dt + \int_{t_1}^{t_2} i_L\,dt + \int_{t_2}^{t_3} i_L\,dt\right) \tag{46}$$

$$\begin{aligned} I_o &= \frac{1}{T_S}\left(\int_{i_{L,0}}^{i_{L,1}} \frac{L i_L}{v_i - v_{ref}}di_L + \int_{i_{L,1}}^{i_{L,2}} \frac{-L i_L}{v_{ref}}di_L + \int_{i_{L,2}}^{i_{L,3}} 0\;di_L\right) \\ &= \frac{1}{T_S}\frac{L v_i {i_{L,1}}^2}{2 v_{ref}\left(v_i - v_{ref}\right)} \end{aligned} \tag{47}$$

Therefore, the switching frequency f_S can be expressed as

$$f_S = \frac{1}{T_S} = \frac{2 v_{ref}\left(v_i - v_{ref}\right)}{L v_i {i_{L,1}}^2} I_o \tag{48}$$

1. σ^1

Thus, the switching frequency for σ^1 can be obtained by substituting (21) into (48),

$$f_S = \frac{1}{T_S} = \frac{2 v_{ref}\left(v_i - v_{ref}\right)}{L v_i\left(\frac{v_{ref} + \Delta_1 - \Psi_1}{R} + \frac{\Psi_1}{c_1}\right)^2} I_o \tag{49}$$

2. σ^2

The switching frequency with σ^2 can be calculated by substituting (36) into (48),

$$f_S = \frac{1}{T_S} = \frac{2 v_{ref}\left(v_i - v_{ref}\right)}{L v_i\left(\frac{v_{ref} + \Delta_2 - \Psi_2}{R} + \sqrt{\frac{\Psi_2}{k_1}}\right)^2} I_o \tag{50}$$

D. Simplified expressions of v_{avg}, v_{ripple}, and f_S

Eqs. (29), (30), and (49) give the expressions of v_{avg}, v_{ripple}, *and* f_S for converters with σ^1, while Eqs. (40), (41), and (50) give the expressions for converters with σ^2. In order to study their relationships with the load current, some simplifications have been adopted and discussed in the following.

1. σ^1

By substituting $[v_{o,0}, i_{L,0}] = [v_{o,\min}, 0]$ into (5) and assuming $v_{o,\min} \approx v_{avg}$,

$$v_{avg} = c_1 I_o + v_{ref} - \Delta_1 \tag{51}$$

where $I_o = \frac{v_{avg}}{R}$.

By substituting $v_{o,1}$ with v_{avg} in (20) and comparing the result with (51), it gives

$$\Psi_1 = 2\Delta_1 - c_1 I_o \tag{52}$$

Then, by putting (52) into (28), it gives

$$v_{ripple} = \frac{v_i\,\alpha}{v_{ref}}\left(c_1 I_o - 2\Delta_1\right)^2 \tag{53}$$

By putting (20) and (52) into (21), it can be shown that

$$i_{L,1} = \frac{2\Delta_1}{c_1} \tag{54}$$

Thus, by substituting (54) into (48), the switching frequency can be expressed as,

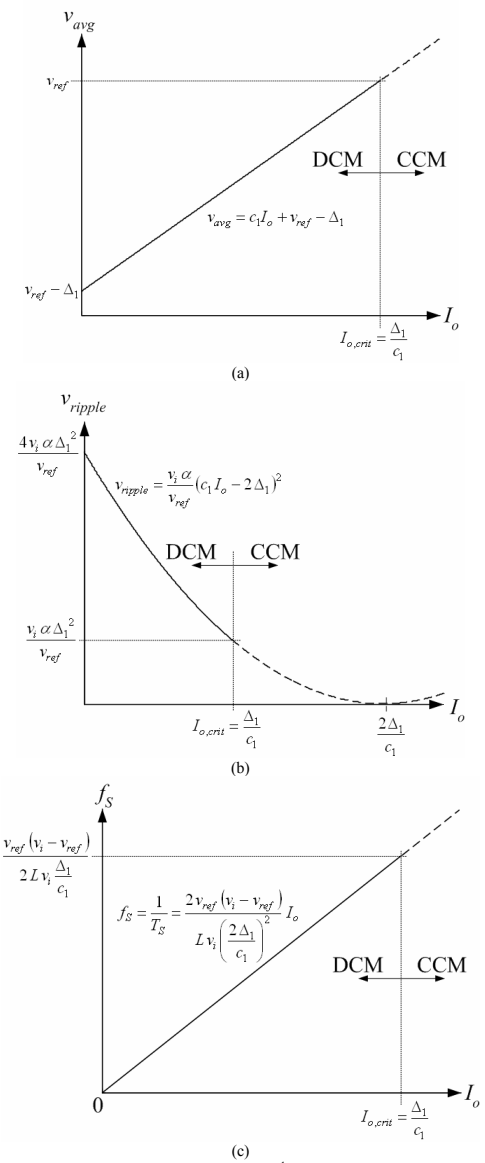

Fig. 4 Steady-state characteristics of converters with σ^1. (a) v_{avg}. (b) v_{ripple}. (c) f_S.

$$f_S = \frac{1}{T_S} = \frac{2 v_{ref}\left(v_i - v_{ref}\right)}{L v_i\left(\frac{2\Delta_1}{c_1}\right)^2} I_o \tag{55}$$

Fig. 4 shows the steady-state characteristics against the load current I_o. $I_{o,crit}$ is the value of I_o when $R = R_{crit}^{<1>}$.

2. σ^2

For the ideal values of k_1 and k_2 in (8), $k_2 - \beta k_1 = 0 \Rightarrow \Phi_2 = 0$. Thus,

$$\Psi_2 = \frac{2\Delta_2}{1+\beta} \tag{56}$$

By substituting $v_{o,1}$ with v_{avg}, and (35) into (36), (40), and (41), it can be shown that

$$i_{L,1} = I_o + \sqrt{\frac{2\Delta_2}{k_1(1+\beta)}} = I_o + \sqrt{\frac{2\Delta_2}{k_1 + k_2}} \tag{57}$$

and

$$v_{avg} = v_{ref} + \left(\frac{v_i}{v_{ref}}\frac{\beta}{1+\beta} - 1\right)\Delta_2 \tag{58}$$

and

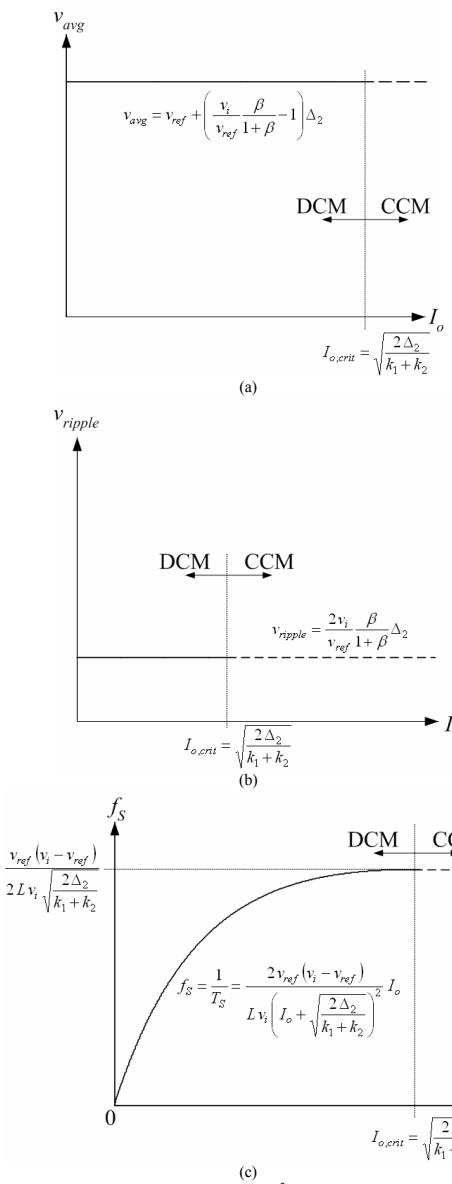

Fig. 5 Steady-state characteristics of converters with σ^2. (a) v_{avg}. (b) v_{ripple}. (c) f_S.

$$v_{ripple} = \frac{2v_i}{v_{ref}}\frac{\beta}{1+\beta}\Delta_2 \tag{59}$$

Thus, by putting (57) into (48), the switching frequency can be expressed as

$$f_S = \frac{1}{T_S} = \frac{2v_{ref}(v_i - v_{ref})}{Lv_i\left(I_o + \sqrt{\frac{2\Delta_2}{k_1+k_2}}\right)^2} I_o \tag{60}$$

Fig. 5 shows the steady-state characteristics against the load current I_o.

E. Effects of r_C on the Operating Mode

As illustrated in Fig. 6(a), the on- and off-state trajectories vary with r_C. Figs. 6(b) and (c) show the shifts of the steady-state trajectories with different values of r_C for the converter with σ^1 and σ^2, respectively. The analyses are based on the component values tabulated in Table I. The converter changes from DCM to CCM, as r_C increases. Moreover, the steady-state on and off trajectories will move along the same path and become a straight line. Similar to the method described in [3], a straight line of slope m connecting the two switching instants t_0 and t_1 can be expressed as

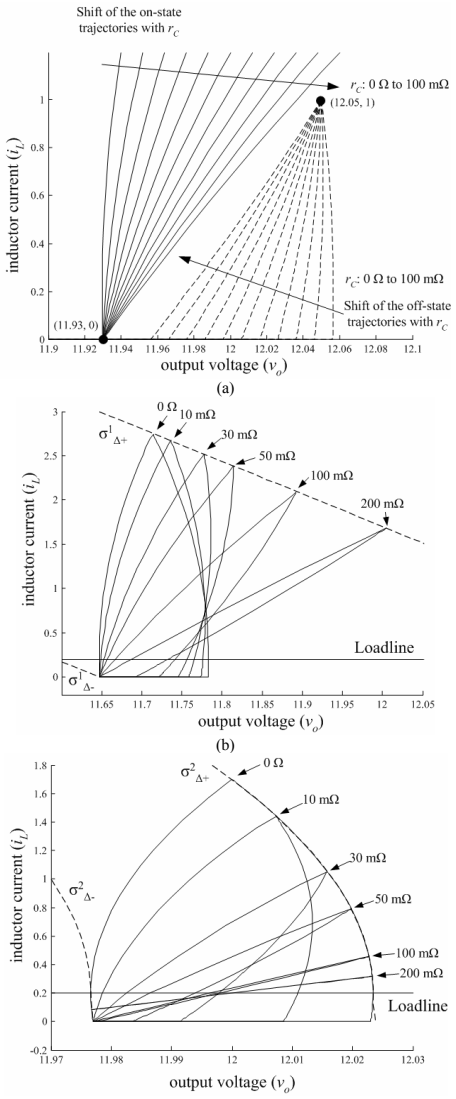

Fig. 6 Shift of steady-state trajectories against r_C. (a) on-state and off-state trajectories. (b) Converter trajectories with σ^1. (c) Converter trajectories with σ^2.

$$m = \frac{i_{L,1} - i_{L,0}}{v_{o,1} - v_{o,0}} = \frac{R + r_C}{R\, r_C} \tag{61}$$

By putting $i_{L,0} = 0$ and assuming that the line passes through the point $\{v_{ref}, v_{ref}/R\}$ in CCM, (61) can be expressed as

$$r_C = \left(\frac{v_{ref}}{v_{o,0}} - 1\right)R \tag{62}$$

Thus, the critical value of r_C, $r_{C,crit}$, that the converter starts operating in CCM can be calculated by substituting (19) into (62) for σ^1, and (34) into (62) for σ^2. For σ^1,

$$r_{C,crit}^{<1>} = R\left(\frac{\Delta_1}{v_{ref} - \Delta_1}\right) - c_1\left(\frac{v_{ref}}{v_{ref} - \Delta_1}\right) \tag{63}$$

For σ^2,

$$r_{C,crit}^{<2>} = \frac{2k_2 v_{ref}}{R\left(1 - \sqrt{1 - \frac{4k_2}{R^2}\left(v_{ref} - \Delta_2\right)}\right)} - R \tag{64}$$

IV. Parametric Variations on the Converter Characteristics

The components L and C, and v_i are subject to variation

$$v_i = v_{i,N}\left(1 + \delta_1\right) \tag{65}$$

$$L = L_N\left(1+\delta_2\right) \tag{66}$$

$$C = C_N\left(1+\delta_3\right) \tag{67}$$

where $v_{i,N}$, L_N, and C_N are the nominal values of v_i, L and C, respectively, δ_1, δ_2 and δ_3 are the fractional variations of v_i, L and C, respectively. Sensitivities of v_{avg}, v_{ripple}, *and* f_S to δ_1, δ_2 and δ_3 are based on eqs. (51), (53), (55) for σ^1 and eqs. (58)-(60) for σ^2.

A. With σ^1

By substituting (65)-(67) into (51), (53) and (55), the % change of v_{avg}, v_{ripple}, *and* f_S from its nominal value are

$$\%\Delta v_{avg} = \frac{v_{avg}\left(v_i, L, C\right) - v_{avg}\left(v_{i,N}, L_N, C_N\right)}{v_{avg}\left(v_{i,N}, L_N, C_N\right)} = 0 \tag{68}$$

$$\%\Delta v_{ripple} = \frac{v_{ripple}(v_i, L, C) - v_{ripple}(v_{i,N}, L_N, C_N)}{v_{ripple}(v_{i,N}, L_N, C_N)} = \xi_1(\delta_1, \delta_2, \delta_3) \tag{69}$$

$$\%\Delta f_S = \frac{f_S(v_i, L, C) - f_S(v_{i,N}, L_N, C_N)}{f_S(v_{i,N}, L_N, C_N)} = \xi_2(\delta_1, \delta_2, \delta_3) \tag{70}$$

where $D_N = v_{ref} / v_{i,N}$ is nominal duty cycle, $\xi_1(\delta_1, \delta_2, \delta_3) = \dfrac{(1+\delta_1)(1+\delta_2)(1-D_N)}{(1+\delta_3)(1+\delta_1-D_N)} - 1$, and $\xi_2(\delta_1, \delta_2, \delta_3) = \dfrac{(1+\delta_1)-D_N}{(1+\delta_1)(1+\delta_2)(1-D_N)} - 1$.

B. With σ^2

By substituting (65)-(67) into (58), (59) and (60), the % change of v_{avg}, v_{ripple}, *and* f_S from its nominal value are

$$\%\Delta v_{avg} = \xi_3(\delta_1, \delta_2, \delta_3)\ \frac{\Delta_2}{v_{ref}} \tag{71}$$

$$\%\Delta v_{ripple} = \xi_3(\delta_1, \delta_2, \delta_3) \tag{72}$$

$$\%\Delta f_S = \xi_2(\delta_1, \delta_2, \delta_3) \tag{73}$$

where $\xi_3(\delta_1, \delta_2, \delta_3) = \dfrac{(1+\delta_1)(1+\delta_2)}{(1+\delta_1)(1+\delta_3)+D_N(\delta_2-\delta_3)} - 1$.

By using the function of "fmincon" on MATLAB, Fig. 7 shows the maximum value of ξ_1, ξ_2, and ξ_3 at different duty cycle D_N from 0.1 to 0.7, where v_i is subject to a maximum variation of ±20% (i.e., $\delta_1 \in$ [-0.2, +0.2]) , and L and C are subject to a maximum variation of ±10% (i.e., δ_2, $\delta_3 \in$ [-0.1, +0.1]).

v_{avg} in σ^2 [eq. (71)] is sensitive to the component variation, as compared with σ^1 [eq. (68)]. It is mainly because σ^2 is dependent on the component values, while σ^1 is explicitly determined. However, as shown in (71), $\Delta_2 << v_{ref}$, the variation of v_{avg} with respect to parametric variation is very small.

Compared (69) with (72), the variation of v_{ripple} in σ^2 is much less than that of σ^1. The former one only varies between -15% and +20%, while the latter one can be up to 200%.

Compared (70) with (73), the frequency variations in the two switching surfaces are the same.

V. Large-Signal Characteristics

The large-signal analysis method shown in [3] is based on assuming that the hysteresis band is zero. As DCM is introduced by nonzero hysteresis band, the large-signal characteristics are studied by considering the transition boundaries of the upper and lower bounds. The transition boundaries with σ^1 and σ^2 are shown in Fig. 8. As illustrated in Fig. 8(a), the transition boundaries for $\sigma^1_{\Delta-}$ and $\sigma^1_{\Delta+}$ are all in the reflective regions (as shown in Fig. 5(a) in [3]) and thus the converter is in the sliding mode. The transition boundaries for

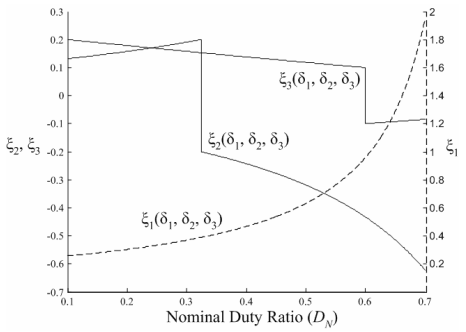

Fig. 7 Maximum values of ξ_1, ξ_2, and ξ_3 at different duty cycle D_N.

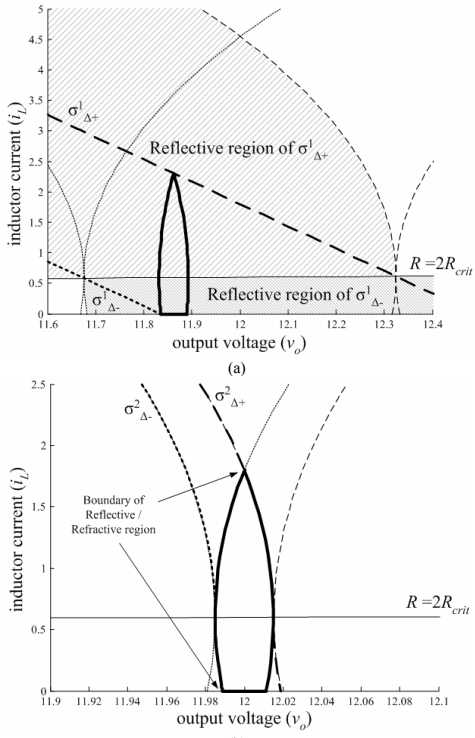

Fig. 8 Transition boundaries of the upper and lower bounds. (a) σ^1. (b) σ^2.

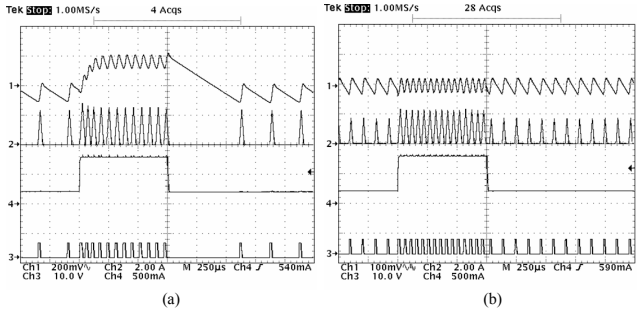

Fig. 9 Transient response of buck converter when load change from 0.2 A (2.4 W) to 0.8 A (9.6 W), and vice versa. [Ch2: i_L(2 A/div), Ch3: v_{gate}(10 V/div), Ch4: i_{out}(500 mA/div)] (Timebase: 250μs/div) (a) σ^1 [Ch1: v_{out}(200 mV/div)]. (b) σ^2 [Ch1: v_{out}(100 mV/div)].

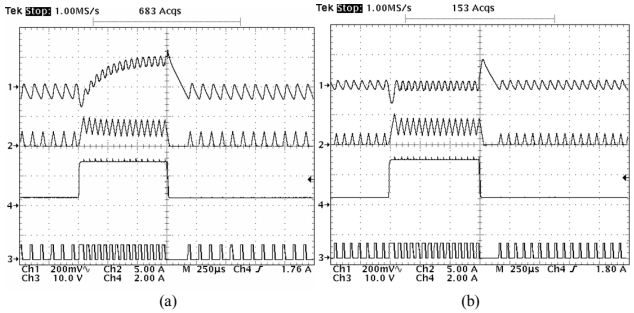

Fig. 10 Transient response of buck converter when load change from 0.5 A (6 W) to 3 A (36 W), and vice versa. [Ch1: v_{out}(200 mV/div), Ch2: i_L(5 A/div), Ch3: v_{gate}(10 V/div), Ch4: i_{out}(2 A/div)] (Timebase: 250μs/div) (a) σ^1. (b) σ^2.

$\sigma^2_{\Delta-}$ and $\sigma^2_{\Delta+}$ are similar to the ones in CCM and are always on the boundaries of reflective and refractive regions [Fig. 8(b)]. It exhibits the advantages of providing near-optimum transient response to large-signal disturbances. Detailed discussions can be found in [3].

TABLE I
COMPONENT VALUES OF THE PROTOTYPE

Parameter	Value
v_i	24 V
v_{ref}	12 V
L	100 μH
C	400 μF
R	60 Ω
c_1	0.2702
$\{k_1, k_2\}$	{0.0104, 0.0104}
f_S	20 kHz
Δ_1	405.3 mV
Δ_2	23.4 mV

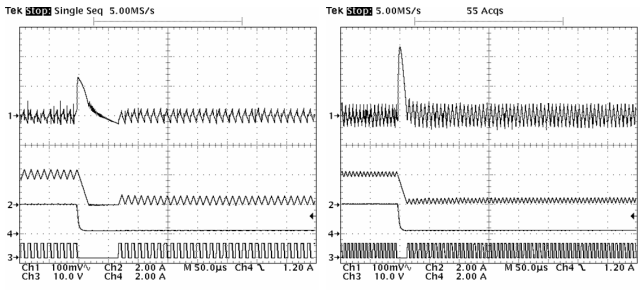

Fig. 11 Transient response of buck converter when I_o is changed from 2 A (24 W) to 0.2 A (2.4 W). [Ch1: v_{out}(100 mV/div), Ch2: i_L(2 A/div), Ch3: v_{gate}(10 V/div), Ch4: i_{out}(2 A/div)] (Timebase: 50μs/div). (a) r_C = 100 mΩ. (b) r_C = 200 mΩ.

VI. EXPERIMENTAL VERIFICATIONS

A buck converter with the component values tabulated in Table I is studied. The parameter c_1 in σ^1 is obtained by optimizing the startup transient as in [3]. Fig. 9 shows the transient responses with σ^1 and σ^2, respectively, when the output load is changed from 0.2 A (2.4 W) to 0.8 A (9.6 W), and vice versa. It can be seen that the output has a voltage drift in σ^1 and does not appear in σ^2. σ^1 takes about 200μs to settle, while σ^2 seems to have no transient period. Fig. 10 shows the converter response when it is subject to a large-signal change that the load is changed from 0.5 A (6 W) to 3 A (36 W), and vice versa. The operating mode of the converter is switched between DCM and CCM. The converter with σ^1 takes more than 500μs to settle from 0.5 A to 3 A and takes 200μs from 3 A to 0.5 A. The one with σ^2 takes about 50μs to settle from 0.5 A to 3 A and takes 150μs from 3 A to 0.5 A. Thus, σ^2 exhibits better dynamic response than σ^1. With the same control law, the converter with σ^2 can regulate the converter in both modes and there is no voltage drift. The dynamic response with σ^2 is much better than that of σ^1. Fig. 11(a) and (b) shows the converter output with r_C equal to 100 mΩ and 200 mΩ, respectively. The output current is changed from 2 A to 0.2 A. The equivalent value of R when I_o = 0.2 A is 60 Ω. Based on (64), $r_{C,crit}^{<2>}$ = 115 mΩ. When r_C = 100 mΩ, the converter at I_o = 0.2 A is close to CM [Fig. 11(a)]. When r_C = 200 mΩ, the converter at I_o = 0.2 A is in CCM [Fig. 11(b)]. This confirms the discussion in Sec. III. Fig 12 shows the measurement results of v_{avg}, v_{ripple}, *and* f_S with σ^1 and σ^2, as compared with eqs. (29), (30), and (49) for σ^1 and eqs. (40), (41) and (50) for σ^2. Theoretical predictions are in good agreement with experimental results.

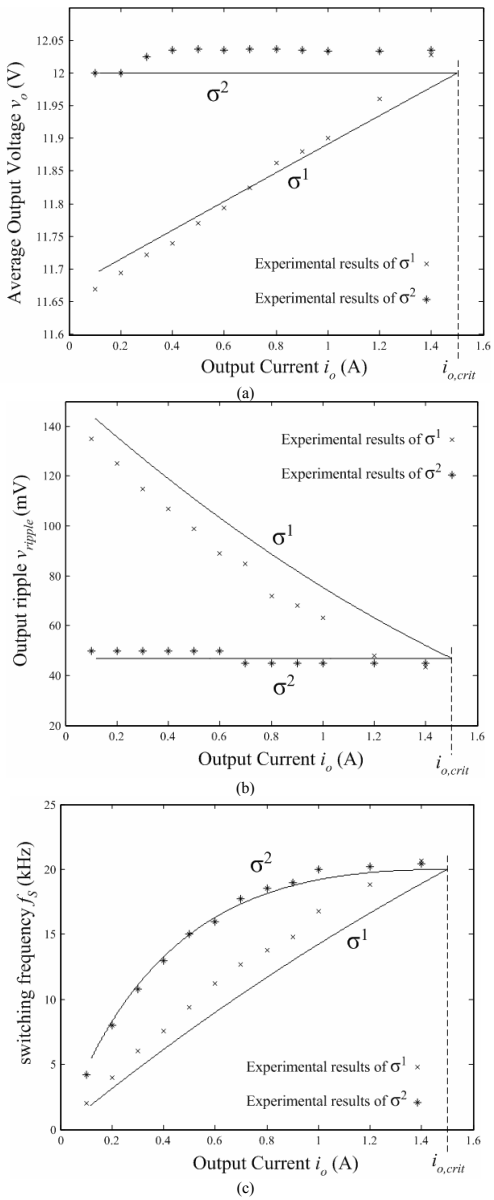

Fig. 12 Experimental measurement of the steady-state characteristics of converters with σ^1 and σ^2. (a) v_{avg}. (b) v_{ripple}. (c) f_S.

VII. CONCLUSION

A comparative study on the static and dynamic behaviors of buck converters operating in DCM with the first-order and second-order switching boundaries have been examined. Detailed mathematical analyses have been given and have been supported by experimental measurements. Generally, converters with the second-order surface are found to give better dynamic responses and than the ones with the first-order surface.

REFERENCES

[1] P.T. Krein, *Elements of Power Electronics*, Oxford University Press, 1998, Chap. 17.

[2] P.T. Krein, *Nonlinear Phenomena in Power Electronics: Attractors, Bifurcation, Chaos, and Nonlinear Control*. New York: IEEE Press, 2001, Chap. 8.

[3] K.K.S. Leung and H.S.H. Chung, "A Comparative Study of the Boundary Control of Buck Converters Using First- and Second-Order Switching Surfaces - Part I: Continuous Conduction Mode," in *Record, IEEE Power Electron. Spec. Conf.,* Recife, Brazil, June 2005.